ELSEVIER

Neuroscience Letters 322 (2002) 49–52

Neuroscience Letters

www.elsevier.com/locate/neulet

The effect of different morphological sampling criteria on the fraction of bursting cells recorded in the rat subiculum in vitro

L. Menendez de la Prida*, F. Suarez, M.A. Pozo

Brain Mapping Unit, Instituto Pluridisciplinar, Universidad Complutense de Madrid, Paseo Juan XXIII, 1, Madrid 28040, Spain

Received 6 November 2001; received in revised form 10 January 2002; accepted 10 January 2002

Abstract

In spite of the large variability of the fraction of bursting cells reported in the subiculum (from 54 to 100%), this structure has been considered as intrinsically bursting. Here, using visually assisted whole-cell recordings and Neurobiotin labeling in vitro, we correlated the electrophysiological firing modes of subicular cells (bursting, regular-spiking and fast-spiking) with their morphological characteristics (somatic size and shape). We then examined how different morphological sampling criteria for patching affect cell classification. We found a dramatic variability in the fraction of bursting cells, which ranged from 30 to 76% depending on the sampling criteria. We discuss the implications of these findings for the notion of the subiculum as an intrinsically bursting structure.

Keywords: Subiculum; Bursting; Morphology; Sampling bias; Whole-cell recordings; Slices

Classification of neuronal types has traditionally been useful in relating neural form to function. For more than a century, morphologists have been classifying cells according to their somatic shape, dendritic morphology and projecting patterns [10]. With the development of recording techniques, electrophysiological classification of cell types became possible, showing a large diversity of firing modes [2,4–6]. However, the choice of electrode can influence the sample of the cells and bias the study towards a particular cell type [11,14]. This may produce controversial results in classification studies.

The subiculum is an example where the proportion of a particular cell class, i.e. the bursting cells, is not clear. Using sharp electrodes, various laboratories have reported a fraction of bursting cells that ranges from 69 to 100% [3,7–9,13,15], supporting the view of the subiculum as a bursting structure. Nevertheless, using similar recording techniques a lower fraction of bursting cells has been reported, i.e. 54% [1]. In a subsequent study, Green and Totterdell found that the fraction of bursting cells varied across the longitudinal and vertical axes of the subiculum [3], suggesting that the wide variability may be due to a spatial bias effect. Nevertheless, a recent work using whole-cell recordings from pyramidal cells again reported a large fraction of bursting cells independent of the vertical subicular axes [12]. Here, we explored whether there is a sampling bias affecting cell classification in the subiculum and looked for estimates of bursting cell fraction using no a priori morphological sampling criteria for patching. We classified the cellular populations of the subiculum according to their electrophysiological firing modes and correlated them with their morphological characteristics (somatic size and shape). We then examined how different morphological sampling criteria affect the fraction of bursting cells recorded in the subiculum.

We recorded from subicular neurons in combined horizontal hippocampal/entorhinal cortical slices (350 μm) obtained from 17–22-day-old Wistar rats. Briefly, rats were decapitated under slight ether anesthesia and their brains quickly removed and chilled in cold artificial cerebrospinal fluid (ACSF) containing (in mM): 125 mM NaCl, 3 mM KCl, 1 mM $MgSO_4$, 1.2 mM NaH_2PO_4, 2 mM $CaCl_2$, 22 mM $NaHCO_3$, 10 mM glucose (pH 7.4). Somatic whole-cell recordings were made using patch pipettes of 4–6 MΩ when filled with (in mM): 131 K-gluconate, 6 KCl, 1 $MgCl_2$, 1 NaCl, 1 EGTA, 5 HEPES, 2 K_2ATP, 0.3 NaGTP; pH 7.3 adjusted with KOH and osmolarity 290–300 mOsm. Cells were loaded with Neurobiotin (0.1–0.5%) and processed using 3,3′-diaminobenzidine reaction for subsequent morphological reconstruction. Since the fraction of bursting

* Corresponding author. Tel.: +34-91-394-3295; fax: +34-91-394-3264.

E-mail address: liset@pluri.ucm.es (L. Menendez de la Prida).

0304-3940/02/$ - see front matter
PII: S0304-3940(02)00085-X

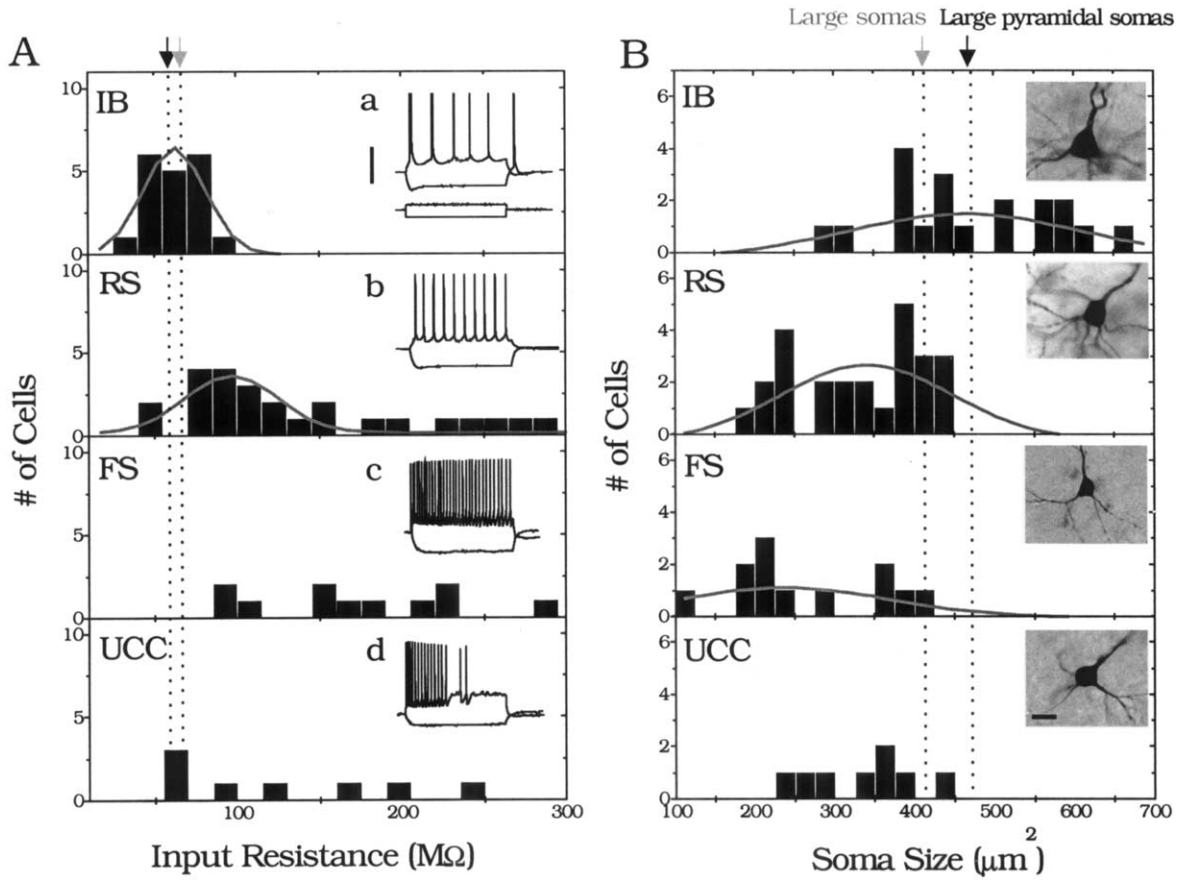

Fig. 1. (A) Distribution of input resistance across the electrophysiological groups: IB, intrinsic bursting; RS, regular-spiking; FS, fast-spiking; UCC, unclassified cells. Insets on the right show representative cell responses of each group to depolarizing and hyperpolarizing current pulses of 500 ms duration and ±0.2 nA amplitude. Vertical scale bar: 20 mV. (B) Distribution of somatic size (computed as the product of somatic width and length) across the electrophysiological groups. Insets on the right show representative Neurobiotin labeled cells from each group. Horizontal scale bar: 25 μm.

cells could vary across the vertical (alveus-hippocampal fissure) and longitudinal (CA1-entorhinal cortex) axes [3], recordings were made within 250–500 μm from the alveus and 300–800 μm from the CA1 region. Whole-cell recordings in current-clamp mode were made using an Axoclamp 2B amplifier (Axon Inst.), digitized (Digidata 1322A, Axon Inst.) and stored on disk at a 10 kHz sampling frequency.

We initially patched cells using no a priori morphological sampling criteria, i.e. we patched the first healthy cell found by visual inspection ($n = 64$ cells). As previously described, cells were electrophysiologically classified as bursting and non-bursting, according to their firing responses to depolarizing current pulses of 500 ms duration [1,3,7–9,13,15]. Bursting (IB, $n = 19$) cells typically fired one or more bursts of action potentials (Fig. 1Aa). Non-bursting cells included regular-spiking (RS, $n = 25$, Fig. 1Ab) and fast-spiking cells (FS, $n = 12$, Fig. 1Ac). A number of cells remained unclassified, as they did not match any clear firing pattern ($n = 8$, Fig. 1Ad). Electrophysiologically, IB cells had lower input resistance (R_N) and membrane time constant (τ_m) compared to non-bursting cells (Student's t-test, $P < 0.05$, Table 1). Morphologically, the somata of bursting cells were more pyramidal and larger than those of non-bursting cells (Table 1). The majority of IB and RS cells had both local and projecting axon collaterals. The somata of FS cells were typically ovoid-shaped with no clear main dendritic branch. FS cells were morphologically identified as local circuit interneurons.

Both R_N and somatic size (computed as the product of the somatic width and length) were differently distributed across the electrophysiological groups. As shown in histograms of Fig. 1A,B, the distributions of R_N and somatic size of IB and RS cells were different ($P < 0.05$, Student's t-test). FS cells tended to have lower values of somatic size, which were distributed differently from those of IB cells but not from those of RS cells (Fig. 1B). The distribution of R_N in FS cells was random (Fig. 1A). Both R_N and somatic size data from unclassified neurons were also randomly distributed (Fig. 1A,B). We found input resistance to be inversely correlated with somatic size (coefficient of correlation $R = 0.61$), showing a predictable relationship useful for cell classification [5]. All this indicates a morphological separation, with bursting cells being larger than RS and FS cells.

Table 1
Passive and morphological properties of subicular cells according to different morphological sampling criteria

	IB	RS	FS	Unclassified
No morphological sampling criteria[a]				
Resting membrane potential (RMP) (mV)	−61 ± 6	−64 ± 7	−66 ± 6	−55 ± 6
R_N (MΩ)	62 ± 16*[b]	137 ± 71*,**	198 ± 110	125 ± 69
τ_m (ms)	8.2 ± 2.3*	12.1 ± 2.5*	16.6 ± 4.9	19.8 ± 5.8
Soma shape (pyramidal/total)	14/19	15/25	0/12	2/8
Soma size (μm^2)	467 ± 104*	333 ± 79*,***	262 ± 98	333 ± 64
n	19	25	12	8
Visually selected cells (large somata)				
R_N (MΩ)	69 ± 31	81 ± 14**	96 ± 24	65 ± 21
Soma size (μm^2)	401 ± 54	360 ± 68***	414 ± 17	368 ± 22
n	13	4	2	2
Visually selected cells (large pyramidal somata)				
R_N (MΩ)	62 ± 32	82 ± 32**	–	–
Soma size (μm^2)	495 ± 74	392 ± 10***	–	–
n	14	9		

[a] We patched the first cell that came across under visual guidance.
[b] *$P < 0.05$ for IB vs. RS. **$P < 0.05$ for input resistance (R_N) in original vs. visually selected RS cells. ***$P < 0.05$ for somatic size in original vs. visually selected RS cells.

In the absence of a priori morphological sampling criteria we found that bursting cells constituted a low proportion of the total recorded cells in a constrained area of the subicular cell layer (30%, Table 2). This proportion increased to 34% if unclassified cells were not included, and to 36% if interneurons were left out. If both interneurons and unclassified cells were excluded, bursting cells constituted 43% of all recorded neurons.

Considering only the morphologically identified pyramidal neurons, bursting cells constituted 45% (Table 2), which increased to 48% if unclassified cells were not included. Similarly, if only morphologically identified ovoid somata were selected, bursting cells represented 15% of the population. To further explore the effect of a possible sampling bias in the proportion of bursting cells we used different a priori criteria to select cells for patching.

We recorded from a second set of 21 visually selected cells with large somata. Using this criterion we found 13 bursting cells (62%), four RS (19%) and two FS cells, while two cells remained unclassified (Table 2). If neither interneurons nor unclassified cells were considered, bursting cells constituted 76% of this second set of cells. The input resistance and somatic size of these cells (see Table 1) lie at one tail of the original statistical distributions of RS cells recorded using no sampling criteria ($P < 0.05$, Fig. 1A,B, gray arrows). On the contrary, neither R_N nor somatic size of visually selected cells were significantly different compared to the original IB population (Table 1, Fig. 1A,B).

We then recorded from a third set of 23 visually selected cells with large pyramidal somata. With this sampling criterion no FS interneurons or unclassified cells were recorded. We found that bursting cells represented 61% of the population (Table 2). Again, the input resistance and somatic size of these cells lie at the tail of the original distributions of RS cells, being not significantly different from the original IB cells ($P < 0.05$, Fig. 1A,B, black arrows).

The largest proportion of subicular bursting cells has been reported in studies using sharp electrodes. In slices from Sprague–Dawley rats, Taube found that 69% of cells were bursting [15], similar to Green and Totterdell in Wistar rats [3] and Steward and Wong in guinea-pig [13]. However, Mattia et al. reported a bursting cell fraction of 100% [8] and Mason 75% [7]. One exception was reported by Behr et al. [1], who found a 54% fraction of bursting cells. Using similar recording techniques, Green and Totterdell [3] systematically analyzed the morphology of IB and RS cells

Table 2
Comparison of the effect of different sampling criteria in the proportion of cellular types

Sampling criteria	*N*	IB (%) (*n*)	RS (%) (*n*)	FS (%) (*n*)	Unclassified (%) (*n*)
No sampling criteria	64	30 (19)	39 (25)	19 (12)	12 (8)
Morphologically identified cells (pyramidal somata)	31	45 (14)	48 (15)	–	7 (2)
Morphologically identified cells (ovoid somata)	33	15 (5)	30 (10)	36 (12)	18 (6)
Visually selected cells (large somata)	21	62 (13)	19 (4)	10 (2)	10 (2)
Visually selected cells (large pyramidal somata)	23	61 (14)	39 (9)	–	–

and found that bursting cells were of the pyramidal type. They also noted that IB cells had lower R_N than RS cells [3,13]. Using visually-assisted whole-cell recordings, Staff et al. [12] found 68% bursting cells in 14–48-day-old rats. Nevertheless, these authors only selected pyramidal cells for patching, and found no particular morphological difference between IB and RS cells. In the majority of these studies FS interneurons were not included when computing the bursting cell fraction. Except in Ref. [3], unclassified cells were not reported.

Since large cells make bigger physical targets for blind recordings, it is possible that sharp electrodes could be biased towards larger cells in a particular region [11]. Patch recordings are also biased toward specific cell types depending on pipette tip size and visual sampling criteria. Subicular bursting cells were larger than non-bursting cells. Using visual criteria to select larger cells for patching we found a fraction of IB cells (from 61 to 76%, only including RS and IB cells) that is similar to that reported using sharp electrodes (54–100%) and whole-cell recordings with similar sampling criteria (68%) [12].

The large proportion of bursting cells reported by various laboratories has supported the view of the subiculum as an intrinsically bursting structure. By using no morphological sampling criteria we found that only 30% of subicular cells were bursting, while 39% were RS. FS interneurons and unclassified cells together represented 31% of the population. This electrophysiological diversity of firing patterns in a constrained area of the subicular cell layer suggests that the subiculum can be much more complex than originally thought. We also propose that the different percentage of subicular bursting cells reported using sharp electrodes [1,7–9,13,15] might come from a sampling bias effect and not only from a spatial bias [3]. The larger soma size of bursting cells compared to non-bursting cells in the subiculum would shift the probability of impalement in favor of bursting cells. This results in a sampling bias that affects cell classification. Here, we also showed that different visual sampling criteria have dramatic consequences for cell classification using whole-cell recordings, so care should be taken in choosing criteria, especially when results are generalized.

This work was supported by the Comunidad Autónoma de Madrid (Grant 08.5/0023.3/99) and Ministerio de Ciencia y Tecnología (Grant SAF2000-0140). L.M.P. is supported by the Comunidad Autónoma de Madrid. We thank L. Borg-Graham, M. Maravall and F. Viana for comments and discussion and N. Lauzurica for technical assistance.

[1] Behr, J., Empson, R.M., Schmitz, D., Gloveli, T. and Heinemann, U., Electrophysiological properties of rat subicular neurons in vitro, Neurosci. Lett., 220 (1996) 41–44.
[2] Connors, B.W., Gutnick, M.J. and Prince, D.A., Electrophysiological properties of neocortical neurons in vitro, J. Neurophysiol., 48 (1982) 1302–1320.
[3] Green, J.R.T. and Totterdell, S., Morphology and distribution of electrophysiologically defined classes of pyramidal and nonpyramidal neurons in rat ventral subiculum in vitro, J. Comp. Neurol., 380 (1997) 395–408.
[4] Hubel, D.H., Tungsten microelectrode for recording from single units, Science, 125 (1957) 549–550.
[5] Kawaguchi, Y., Groupings of nonpyramidal and pyramidal cells with specific physiological and morphological characteristics in rat frontal cortex, J. Neurophysiol., 69 (1993) 416–431.
[6] Llinas, R., The intrinsic electrophysiological properties of mammalian neurons: insights into central nervous system function, Science, 242 (1988) 1654–1664.
[7] Mason, A., Electrophysiology and burst-firing of rat subicular pyramidal neurons in vitro: a comparison with area CA1, Brain Res., 600 (1993) 174–178.
[8] Mattia, D., Hwa, G.G.C. and Avoli, M., Membrane properties of rat subicular neurons in vitro, J. Neurophysiol., 70 (1993) 1244–1248.
[9] Mattia, D., Kawasaki, H. and Avoli, M., In vitro electrophysiology of rat subicular bursting neurons, Hippocampus, 7 (1997) 48–57.
[10] Ramon y Cajal, S., Histologie du Système Nerveux de l'Homme et des Vertébrés, A. Maloine, Paris, 1911.
[11] Sakai, M., Sakai, H. and Woody, C.D., Sampling distribution of morphologically identified neurons of the coronal-pericruciate cortex of awake cats following intracellular injection of HRP, Brain Res., 152 (1978) 329–333.
[12] Staff, N.P., Jung, H., Thiagarajan, T., Yao, M. and Spruston, N., Resting and active properties of pyramidal neurons in subiculum and CA1 rat hippocampus, J. Neurophysiol., 84 (2000) 2398–2400.
[13] Steward, M. and Wong, R.K.S., Intrinsic properties and evoked responses of guinea-pig subicular neurons in vitro, J. Neurophysiol., 70 (1993) 232–245.
[14] Stone, J., Sampling properties of microelectrodes assessed in the cat's retina, J. Neurophysiol., 36 (1973) 1071–1079.
[15] Taube, J.S., Electrophysiological properties of neurons in the rat subiculum in vitro, Exp. Brain Res., 96 (1993) 304–318.